

NJC

Accepted Manuscript



This is an *Accepted Manuscript*, which has been through the Royal Society of Chemistry peer review process and has been accepted for publication.

Accepted Manuscripts are published online shortly after acceptance, before technical editing, formatting and proof reading. Using this free service, authors can make their results available to the community, in citable form, before we publish the edited article. We will replace this *Accepted Manuscript* with the edited and formatted *Advance Article* as soon as it is available.

You can find more information about *Accepted Manuscripts* in the [Information for Authors](#).

Please note that technical editing may introduce minor changes to the text and/or graphics, which may alter content. The journal's standard [Terms & Conditions](#) and the [Ethical guidelines](#) still apply. In no event shall the Royal Society of Chemistry be held responsible for any errors or omissions in this *Accepted Manuscript* or any consequences arising from the use of any information it contains.



www.rsc.org/njc

A Study on the Aromaticity and Magnetic Properties of Triazoleporphyrazines

Ablikim Kerim*

Urumqi Key Laboratory of Green Catalysis and Synthesis Technology, School of Chemistry and Chemical Engineering, Xinjiang University, Urumqi 830046, China

Abstract

The aromaticity of porphyrazine (PA), and its three triazoleporphyrazine (TAP) tautomers as well as their metal complex compounds were examined using the TRE (topological resonance energy) and the MRE (magnetic resonance energy) methods. Their local aromaticity was studied using the BRE (bond resonance energy) and the CRE (circuit resonance energy) methods. The relationship between the global and local aromaticity of TAPs and the position of the substituted nitrogen atom is discussed. The results of these calculations are compared with those provided by other aromaticity indices. Our TRE and MRE results indicate that PA and TAPs possess lower global aromaticity than porphyrin. Our BRE and CRE results show that global aromaticity is closely associated primarily with the five-membered rings which contain the -NH- pyrrolic rings, and the [18]-annulene-like conjugation pathway is not crucial for determining the aromaticity of the entire π -system. Moreover, the circuit-current susceptibility (χ_i) and ring current (RC) were obtained using the graph-theoretical method. The χ_i and RC the results show that all the compounds sustain a diatropic current along the macrocycle and this current is bifurcated when it passes through every five-membered ring. Ring current maps reveal that in the five-membered rings, the ring current prefers to pass through the C-C bond when the ring contains an -NH- group, and through the C-N bond when the ring does not contain an -NH- group.

Key words: Aromaticity; Porphyrazine; Diatropicity; Resonance Energy; NICS(0)

1. Introduction

Porphyrin-related compounds have been the topics of many experimental and theoretical studies¹⁻⁶ due to their unique physical and chemical properties. As important porphyrin analogues, porphyrazine (PA) as well as the triazoleporphyrazine (TAP) represent the family of aromatic compounds⁷. Similar to porphyrins, they both have larger macrocyclic rings and have received extensive attention in recent years because of their peculiar and unconventional chemical and physical properties⁸⁻¹⁰.

Aromaticity is a theoretical concept of great practical importance¹¹. It is one of the most widely used concepts in chemistry. Based on the molecular property from which the aromaticity index is derived, all existent criteria can be divided into a few basic categories such as geometrical^{12,13}, magnetic¹⁴⁻¹⁸, electronic¹⁹⁻²¹, and energetic²²⁻²⁵. However, these indices do not always provide the same results for the same compounds²⁶⁻²⁹. Thus, the reliable prediction of aromaticity is an important remaining task of computational chemistry. Among the magnetic criteria, the most commonly used method of determining aromaticity is the nucleus-independent chemical shift (NICS) method, which is defined as a negative value of magnetic shielding at a given point of the molecule¹⁴. It has been shown that when a ring possesses a negative NICS value, this indicates the presence of an induced diatropic ring current, which is interpreted as aromaticity. On the other hand, when a ring possesses a positive value, this denotes a paratropic ring current and is interpreted as antiaromaticity. The negative NICS value of the

shielding computed at a ring center is denoted as NICS(0); the negative NICS value of the absolute shielding measured 1 Å above the center of the ring is denoted as NICS(1); and the NICS value, computed as the zz component of the NICS tensor 1 Å above the molecular plane, is denoted as NICS(1)_{zz}³⁰⁻³².

The HOMA (harmonic oscillator model of aromaticity) value is a geometric indicator of aromaticity defined using the degree of bond-length alternation^{12,13}.

In a series of papers, Islyaikin et al.³³⁻³⁵ studied the aromatic pathway of porphyrazine and the TAPs using NICS(0) and calculations of HOMA indices. They concluded that the internal cross of the PA and the TAP tautomers is the most aromatic part of these structures and that all five-membered rings make an aromatic contribution to the global aromaticity in TAPs.

In this study, the global aromaticity of PA and of the TAPs was determined by the TRE and MRE methods^{22-25,36}. The local aromaticity is discussed using the BRE and CRE methods³⁷⁻⁴⁰ and compared with other aromatic indices such as the HOMA and the NICS(0) from Islyaikin's previous papers³³⁻³⁵. Based on the results of our calculations, the dominant influencing factors relating to aromaticity are also discussed. Finally, the ring current strength of these compounds is predicted using the graph theory ring current diamagnetism method.

2. Methods of Calculation

Topological resonance energy (TRE) is defined as the difference between the π -electron energy of a conjugated molecule and its hypothetical acyclic reference structure²²⁻²⁵. We have used TRE as a standard measure of global aromaticity. BRE represents the contribution of a given π -bond to the TRE³⁸. BRE for a given π -bond between the atoms p and q is calculated as the difference between the total π -electron energy and the energy of a hypothetical π -system constructed by setting $\beta_{pq} = -i\beta_{pq}$ and $\beta_{qp} = -i\beta_{qp}$, where $\beta_{pq} = \beta_{qp}$ is the resonance integral between the atoms p and q, and i is the square root of -1. Positive BRE values imply aromatic contribution, whereas negative BRE values imply antiaromatic contribution to the given conjugated π -electron system. Thus, BRE for a peripheral π -bond can be used as an indicator of local aromaticity for the ring to which that π -bond belongs³⁹. In general, a molecule that has one or more π -bonds with a large negative BRE is kinetically very unstable⁴⁰. Both of our calculations of the TREs and BREs were carried out within the framework of Hückel molecular orbital theory and they are given in units of $|\beta|$, where β is the standard resonance integral in Hückel theory. It is important to note that not only TRE but also BRE belong to the energetic criteria of aromaticity.

Circuit resonance energy (CRE) represents an energy gain or loss due to cyclic conjugation along a given circuit. The CRE for the i th circuit in a hydrocarbon π -system G is defined as A_i in the following equation^{41,42}:

$$A_i = 4 \prod_{m>n}^{r_i} k_{mn} \sum_j^{\text{occ}} \frac{P_{G-r_i}(X_j)}{P'_G(X_j)} \quad (1)$$

where r_i is a set of carbon atoms that constitute the i th circuit c_i ; k_{mn} is the Hückel parameter for the resonance integral between the π -bond formed by atoms m and n ; m and n run over all π -bonds that belong to r_i ; $G-r_i$ is the subsystem of G , and is obtained by deleting r_i from G ; $P_G(X)$ and $P_{G-r_i}(X)$ are the characteristic polynomials for G and $G-r_i$, respectively; and X_j is the j th largest root of the equation $P_G(X) = 0$; a prime added to $P_G(X)$ indicates the first derivative with respect to X ; j runs over all occupied π molecular orbitals. If some occupied molecular orbitals have the same energies, this formula must be replaced by another⁴³⁻⁴⁵. In fact, A_i was derived from the graph-theoretical formula for ring current

magnetic susceptibility.

The sum of A_i values or CREs over all circuits represents the aromatic stabilization energy of an entire π -system. This sum is termed magnetic resonance energy (MRE), which means a TRE-like quantity derived from the magnetic response of a cyclic π -system^{41,42}:

$$\text{MRE} = \sum_i^G A_i = \sum_i^G \text{CRE}_i / |\beta| \quad (2)$$

A π -electron current induced in each circuit may be called a circuit current (CC). Every circuit is supposed to sustain a π -electron current in the external magnetic field, the intensity of which is given by^{41,42}:

$$I_i = 4.5 I_o A_i \frac{S_i}{S_o} \quad (3)$$

where I_o is the intensity of a π -electron current induced in the benzene ring. S_i and S_o are the areas of r_i and the benzene ring, respectively. In general, ring current (RC) can be obtained by superposing all the CCs^{41,42}. The i -th circuit -current susceptibility (CCS), χ_i , i.e., the contribution of the i th circuit to the ring-current magnetic susceptibility of the entire π -system, can be expressed in the form^{41,42}:

$$\chi_i = 4.5 \chi_o A_i \left(\frac{S_i}{S_o} \right)^2 \quad (4)$$

where χ_o is the ring-current susceptibility of benzene; S_i and S_o are the areas of r_i and the benzene ring, respectively. Positive and negative χ_i values represent diamagnetic and paramagnetic contributions, respectively. The areas for pyrrole, porphyrin, and related species were taken from other literature⁴⁶. Van-Catledge's set of Hückel parameters for heteroatoms⁴⁷ has been used. For the series of indices used herein, the higher the TRE, MRE and CRE values, the more aromatic the rings are. Higher positive values in the HOMA indices and higher negative values in the NICS index all reflect greater aromaticity.

3. Results and Discussion

3.1 Global aromaticity of TAPs

The structure of PA (**1**), the three tautomeric forms (**2a, 2b, 2c**), and the metallated species (**3**) studied here are shown in Figure 1. All these molecules are isoelectronic with porphyrin with 26π -electrons. The TREs and MREs are presented in Table 1. The global HOMA and NICS(0) values reported for these compounds³³⁻³⁴ are also presented in Table 1 for comparison with our results. These were calculated by Islyaikin et al. at the B3LYP/6-31G** density functional level of theory and used

Table 1. TREs and MREs for PA, TAPs and related species.

compounds	TRE $ \beta $	MRE $ \beta $	HOMA	NICS(0)
1	0.1797	0.0908	0.563	-15.5
2a	0.1070	0.0894	0.414	-6.90
2b	0.1549	0.0870	0.575	-14.1
2c	0.2039	0.1272	0.615	-14.8
3	0.1659	0.0965	0.643	-
4	0.3941	0.3227	-	-
porphyrine	0.4322	0.3390	0.652 ^a (0.666) ^a	-16.5 ^a

a) Taken from reference 4.

by them as global aromaticity indices for these compounds³³⁻³⁴. The TRE and MRE for porphyrin are 0.4322β and 0.3390β , respectively⁴⁶. The order of aromaticity predicted by the TRE index is: porphyrin > **4** > **2c** > **1** > **3** > **2b** > **2a**, and the order predicted by the MRE index is: porphyrin > **4** > **2c** > **3** > **1** > **2a** \approx **2b**. It is worth noting that the **1** and the **3** switch places. According to TRE and MRE results, after metallation, we can predict that the aromaticity of **3** will decrease relative to **2c**, whereas it will increase relative to **2b**. The sequence of aromaticity of the three tautomeric structures **2c**>**2b**>**2a** as predicted by the TRE method is fully consistent with the global HOMA and NICS(0) results in Table 1. According to the TRE and MRE results we can predict that **2c** has less than half the aromaticity of porphyrin. However, both the HOMA and NICS(0) values of compound **2c** would make it nearly as aromatic as porphyrine. It is evident that the HOMA and NICS(0) methods overestimate the global aromaticity of these compounds. From the order of global aromaticity we can conclude that the replacement by the triazole unit of those five-membered rings which do not contain an -NH- group, leads to an increase in the aromaticity of the macrocycle. However, the replacement of those five-membered rings which do contain an -NH- group, leads to a decrease in the aromaticity of the macrocycle.

That the aromaticity of these compounds is lower than porphyrin can be explained in the following manner. According to Gimarc's topological charge stabilization (TCS) rule⁴⁸, the heteroatomic molecules are stabilized when more electronegative atoms than carbon atoms are placed in those positions where the atoms of the uniform reference frame (URF) have the highest electron charge. The URF of these compounds is presented in Fig. 2. In order to distinguish them from each other, the four five-membered rings are assigned the different symbols A, B, C, and D. These are also utilized in Fig. 2. Nitrogen has greater electronegativity than carbon. Four nitrogen atoms are located at the positions (21, 22, 23, 24) which have the highest charge density in the URF. These four nitrogen atoms conform to the TCS rule and are enough to stabilize this system. Thus, porphyrin exhibits larger aromaticity than PA, the TAPs, and the URF. However, the positions 5, 10, 15, and 20 in the URF exhibit the smallest charge density. Another four nitrogen atoms are also located at positions 5, 10, 15, and 20 in the URF, and they do not conform to the TCS rule. It seems likely that compounds **1**, **2a**, **2b**, **2c**, and **3** are greatly destabilized by the presence of the nitrogen atoms in these positions. As can be seen from Table 1, although each of these compounds and the URF are predicted to be aromatic with positive TREs, all of them still exhibit less aromaticity with smaller TREs and MREs than their corresponding URF. That is to say, PA and the TAPs are disobeying the TCS rule and are much less aromatic than their corresponding URF. The aromaticity of these compounds being lower than that of URF, as predicted using the TRE and MRE methods, is fully consistent with the TCS rule. In general, an -NH-group has more electronegativity than an -N= group⁴⁹. According to the TCS rule, an -NH-group, with larger electronegativity, should prefer to be located in that place within the URF which has larger charge density. In reality however, in compound **2a**, the -NH-group is located at position 3, and the -N= group is located at position 21 in the URF. This does not conform to the TCS rule. Namely, the location of the -N= group at position 21 is disadvantageous with respect to aromaticity compared to the -NH-group being in that location. Thus, compound **2a** exhibits the least aromaticity. This clearly explains the relative aromaticities of these isomers as a whole. Recently, Furuta *et al.*⁵⁰ reported the structure and aromaticity from single to multiple *N*-confused porphyrins. The relative aromaticity of such compounds may also be explained in terms of the TCS rule.

3.2 Local Aromaticity of PA and TAPs

In order to determine the delocalized nature of PA and TAPs, we calculated the BREs of the different chemical bonds and the CREs of the conjugated circuits of different sizes. Both quantities can be used as simple indicators of local aromaticity.

3.2.1. BRE of PA and TAPs

The BRE values are included in Figure 1. By comparing the BRE values of **1-3**, we found that except for the C ring in **2a**, all the π -bonds in the five-membered rings which contain an –NH- group exhibit relatively large positive BREs values, whereas the π -bonds in those five-membered rings which do not contain an –NH- group exhibit small positive or negative BREs values in the same molecule. This indicates that the five-membered rings with an –NH- group are the main sources of aromaticity. Moreover, between the two five-membered rings with an –NH- group, we found that within **2a** and **2b**, their A rings exhibit relatively larger positive BRE values than their C rings. This implies that these rings must be making substantial aromatic contributions to the total aromaticity of these compounds. By comparing the BRE values of **1**, **2a**, **2b**, **2c** and **3**, we found that all of the C-N bonds which link two five-membered rings exhibit fairly small positive values. Whereas the C-C bonds in those five-membered rings which do not contain an –NH- group exhibit relatively large negative values. Thus, we may predict that these C-C bonds are the substructures which destabilize the whole molecule. In the case of **4**, all the bonds have positive BRE values, and the highly aromatic C–C bonds in the five-membered rings tend to increase aromaticity due to the formation of 6π -electronic rings. The BREs of **4** are consistent with the view that this molecule exhibits greater relative TRE values than the PA and the TAPs species.

3.2.2. CREs of PA and TAPs

We next examine the CREs of individual circuits within these compounds. As shown in Figure 3, PA has a total of 20 non-identical circuits which are denoted by $r_1, r_2, r_3, \dots, r_{20}$. Four of them are located along the four five-membered rings. The rest of the circuits are located along the macrocycle that encloses the inner cavity. A circuit coterminous with the macrocycle is denoted by r_5 . The CREs values calculated for all circuits in PA and its related species are listed in Table 2. The sum of CREs for all circuits in the π -system was obtained using MRE. A high degree of correlation is found between the TRE and MRE, with a correlation coefficient of 0.9780. This indicates that MRE can be used as a reliable indicator of global aromaticity and that global aromaticity is produced by all possible circuits in the molecule. It is noteworthy that for **1**, **2a** and **2b**, the five-membered circuits (r_1 and r_3) which contain –NH- groups exhibited positive CRE values larger than those of the other circuits, supporting the view that those five-membered rings which contain an –NH- group are dominant contributors to the aromaticity of the entire π -system for these compounds. Whereas the two five-membered circuits without –NH- groups (r_2 and r_4) exhibit the largest negative CREs. We can predict that these two five-membered circuits are the destabilizing substructures of the molecule. The antiaromatic contribution of these two five-membered circuits is associated with the electronegativity of nitrogen atoms at the *meso* positions, which leads to more localized structures. This means that the electron delocalization in the five-membered rings which contain an –NH- group is stronger than that in those which do not contain an –NH- group. For **2c**, not only the r_2 and r_4 circuits, but also the r_1 circuit contribute aromatically to the molecule as a whole. Thus, **2c** exhibits the largest global aromaticity among the TAPs. In the case of **3**, primary stabilization comes from the r_1 circuit. For **4**, primary stabilization comes from the four five-membered circuits r_1 to r_4 . For both **2a** and **2b**, by comparing the CRE values of circuit r_1 and r_3 , we find that due to the presence of the two nitrogen atoms in ring A, the r_1 circuit exhibited larger CRE values than did the r_3 circuit in the same molecule, whereas the CRE

values of the r_2 and r_4 circuits greatly decreased. That is to say, aromaticity increased in the r_1 circuit and decreased in the r_3 circuit, causing **2a** and **2b** to exhibit lower TRE and MRE values than **1**. From these results we can conclude that the presence of nitrogen atoms in the A ring of **2a** and **2b**, serves only to increase the local aromaticity of these circuits. However, since these nitrogen atoms do not conform to the TCS rule, there is a decrease in the global aromaticity of these compounds. The increase in the local aromaticity due to the nitrogen substitution in the five-membered ring might be simply explained in the following manner: when the $-NH-$ group is linked to the $-N=$ group, the structure becomes more aromatic than when the $-NH-$ group is linked to carbon⁴⁹. This observation gives support for the earlier surmise that as the electronegativity differential between the heteroatom and its neighboring atoms is increased, aromaticity decreases¹¹.

Analyzing the trend in the CRE values, which is indicated in Table 2, we find that the r_{11} circuit in **1** and **2b**, the r_8 circuit in **2a**, the r_{14} circuit in **2c**, and the r_5 circuit in **3** and **4**, all of which correspond to the annulene-like substructure, have the largest CRE values among those circuits located along the macrocycle. These are shown in bold in Figure 1. With the exception of **2a**, our results regarding the macrocyclic pathway as predicted by the CRE method are the same as those predicted by Islyaikin et al.^{33,34}. The NICS (0) and HOMA values^{33,44} reported for the individual rings **1-3** are given in Table 2 in parentheses and brackets, respectively. These were by calculated by Islyaikin et al. at the B3LYP/6-31G** density functional level of theory. The A and C ring values of **1**, and the internal

Table 2. CREs, CCs, and CCSs for PA and related species. NICS(0) values (in parenthesis)^a and HOMA^b (in brackets) for all A,B,C, and D rings, and the internal cross and [18] heteroannulene section.

Circuit	CRE/ $ \beta $	CC/ I_0	CCS/ χ_0	Circuit	CRE/ $ \beta $	CC/ I_0	CCS/ χ_0
1				2c			
r_1	0.0376(-11.6)[0.559]	0.1130	0.0754	r_1	0.0536(-5.60)[0.567]	0.1612	0.1078
r_2	-0.0280(-3.84)[0.221]	-0.0842	-0.0563	r_2	0.0318[0.527]	0.0953	0.0636
r_3	0.0376	0.1130	0.0754	r_3	-0.0564[0.143]	-0.1697	-0.1135
r_4	-0.0280	-0.0842	-0.0563	r_4	0.0318[0.527]	0.0953	0.0636
r_5	0.0070[0.942]	0.1646	0.8640	r_5	0.0070[0.948]	0.1655	0.8686
r_6	0.0104	0.2772	1.6397	r_6	0.0018	0.0477	0.2822
r_7	0.0022	0.0580	0.3429	r_7	0.0104	0.2763	1.6343
r_8	0.0104	0.2772	1.6397	r_8	0.0020	0.0543	0.321
r_9	0.0022	0.0580	0.3429	r_9	0.0104	0.2763	1.6343
r_{10}	0.0031	0.0915	0.6022	r_{10}	0.0025	0.0732	0.4816
r_{11}	0.0154[0.767]	0.4572	3.0091	r_{11}	0.0003	0.0092	0.0608
r_{12}	0.0031	0.0915	0.6022	r_{12}	0.0025	0.0732	0.4816
r_{13}	0.0031	0.0915	0.6022	r_{13}	0.0029	0.0849	0.5592
r_{14}	0.0005	0.0151	0.0997	r_{14}	0.0153[0.753]	0.4523	2.9767
r_{15}	0.0031	0.0915	0.6022	r_{15}	0.0029	0.0849	0.5592
r_{16}	0.0044	0.1424	1.0321	r_{16}	0.0004	0.0127	0.0921
r_{17}	0.0007	0.0219	0.1589	r_{17}	0.0040	0.1315	0.9536
r_{18}	0.0044	0.1424	1.0321	r_{18}	0.0004	0.0127	0.0921
r_{19}	0.0007	0.0219	0.1589	r_{19}	0.0034	0.1111	0.8058
r_{20}	0.0009	0.0316	0.2504	r_{20}	0.0005	0.0174	0.1374
2a				3			

r ₁	0.1042(-13.2)[0.922]	0.3127	0.2086	r ₁	0.0693(5.87)[0.835]	0.2087	0.1387
r ₂	-0.0477[-0.145]	-0.1436	-0.0960	r ₂	-0.0106[0.408]	-0.0318	-0.0213
r ₃	0.0177[0.184]	0.0532	0.0355	r ₃	-0.0171[0.376]	-0.0515	-0.0345
r ₄	-0.0360[-0.117]	-0.1084	-0.0725	r ₄	-0.0106[0.408]	-0.0318	-0.0213
r ₅	0.0097[0.891]	0.2297	1.2055	r ₅	0.0208[0.913]	0.4907	2.5726
r ₆	0.0031	0.0817	0.4833	r ₆	0.0075	0.1990	1.1767
r ₇	0.0031	0.0824	0.4876	r ₇	0.0080	0.2121	1.2537
r ₈	0.0147	0.3909	2.3126	r ₈	0.0080	0.2121	1.2537
r ₉	0.0031	0.0824	0.4876	r ₉	0.0080	0.2121	1.2537
r ₁₀	0.0006	0.0163	0.1074	r ₁₀	0.0019	0.0549	0.3612
r ₁₁	0.0043[0.714]	0.1271	0.8362	r ₁₁	0.0019	0.0549	0.3612
r ₁₂	0.0006	0.0163	0.1074	r ₁₂	0.0019	0.0549	0.3612
r ₁₃	0.0045	0.1323	0.8711	r ₁₃	0.0019	0.0557	0.3666
r ₁₄	0.0008	0.0235	0.1549	r ₁₄	0.0019	0.0557	0.3666
r ₁₅	0.0045	0.1323	0.8711	r ₁₅	0.0019	0.0557	0.3666
r ₁₆	0.0007	0.0233	0.1687	r ₁₆	0.0005	0.0149	0.1077
r ₁₇	0.0011	0.0349	0.2531	r ₁₇	0.0008	0.0275	0.1996
r ₁₈	0.0007	0.0233	0.1687	r ₁₈	0.0005	0.0149	0.1077
r ₁₉	0.0000	-0.0007	-0.0053	r ₁₉	0.0005	0.0149	0.1077
r ₂₀	0.0000	-0.0007	-0.0053	r ₂₀	-0.0001	-0.0050	-0.0394
2b				4			
r ₁	0.0765(-12.6)[0.887]	0.2297	0.1532	r ₁	0.0684	0.2061	0.1380
r ₂	-0.0442[0.566]	-0.1330	-0.0889	r ₂	0.0684	0.2061	0.1380
r ₃	0.0287[0.422]	0.0862	0.0575	r ₃	0.0684	0.2061	0.1380
r ₄	-0.0442[0.566]	-0.133	-0.0889	r ₄	0.0684	0.2061	0.1380
r ₅	0.0074[0.943]	0.1758	0.9224	r ₅	0.0283	0.6678	3.5009
r ₆	0.0106	0.2807	1.6604	r ₆	0.0051	0.1353	0.7996
r ₇	0.0022	0.0588	0.3479	r ₇	0.0051	0.1353	0.7996
r ₈	0.0111	0.2942	1.7402	r ₈	0.0051	0.1353	0.7996
r ₉	0.0022	0.0588	0.3479	r ₉	0.0051	0.1353	0.7996
r ₁₀	0.0027	0.0802	0.5279	r ₁₀	0.0002	0.0065	0.0429
r ₁₁	0.0153[0.803]	0.4540	2.9884	r ₁₁	0.0002	0.0065	0.0429
r ₁₂	0.0027	0.0802	0.5279	r ₁₂	0.0002	0.0065	0.0429
r ₁₃	0.0031	0.0925	0.6087	r ₁₃	0.0002	0.0065	0.0429
r ₁₄	0.0005	0.0144	0.0951	r ₁₄	0.0002	0.0065	0.0429
r ₁₅	0.0031	0.0925	0.6087	r ₁₅	0.0002	0.0065	0.0429
r ₁₆	0.0038	0.1223	0.8869	r ₁₆	-0.0002	-0.0068	-0.0491
r ₁₇	0.0006	0.0208	0.1507	r ₁₇	-0.0002	-0.0068	-0.0491
r ₁₈	0.0038	0.1223	0.8869	r ₁₈	-0.0002	-0.0068	-0.0491
r ₁₉	0.0005	0.0146	0.1055	r ₁₉	-0.0002	-0.0068	-0.0491
r ₂₀	0.0006	0.0203	0.1606	r ₂₀	0.0000	-0.0002	-0.0013

a) Taken from reference 33 and 34.

b) Taken from reference 33 and 34.

cross section NICS (0) values, are only qualitatively consistent with our CRE results. Different behavior is observed for rings B and D. According to the standing interpretation using the NICS (0) and HOMA methods, the B and D rings should be aromatic, even though they exhibit negative CRE values. Similar behavior can be found for the other compounds.

3.3 CCs and CCSs of PA and Related Species

The magnetic properties of aromatic compounds, i.e. magnetizabilities, are commonly interpreted on the basis of the well-known ring current model. The CCs and CCSs for PA and its related species, each expressed as a multiple of the benzene value, are provided in Table 2. These quantities can be obtained using eq. 4. In this table, positive and negative values indicate diamagnetic and paramagnetic currents, respectively. All the aromatic circuits predicted by positive CREs make a diamagnetic contribution, whereas the antiaromatic circuits predicted by negative CREs make a paratropic contribution to the molecule. Based on the CC results in Table 2, we can predict that for **1**, large diatropism will arise from circuit r_{11} , while paratropism will arise from circuit r_2 and r_4 . For **2a**, we predict that large diatropism will arise from r_8 , and that paratropism will arise from r_2 and r_4 . For **2b**, we predict that large diatropism will arise from r_{11} , and that paratropism will arise from r_2 and r_4 . For **2c**, we predict that large diatropism will arise from r_{14} , and that paratropism will arise from r_3 . For **3**, we predict that diatropism will arise from r_5 , and that paratropism will arise from r_2 , r_3 and r_4 . For **4**, we predict that large diatropism will arise from r_5 , and that paratropism will arise from r_{16} , r_{17} , r_{18} and r_{19} . Based on the CCS results in Table 2, we can also predict that for **1**, the r_{11} circuit will make the largest diatropic contribution to the CCS value, whereas the most aromatic r_1 circuit will make a markedly smaller diatropic contribution to the CCS value. The intensity of both the CC and CCS values induced in these compounds does not reflect the magnitude of the CRE values correctly. The large circuits, such as r_8 in **2a**, r_{11} in **2b**, r_{14} in **2c**, r_5 in **3** and in **4** are the main sources of both the CC and the CCS values even though these circuits make a relatively small positive contribution to the CRE values. Thus, CCs and CCSs cannot always be used as a reliable indicator of aromaticity for these compounds. This supports the view that five-membered rings which contain an –NH– group are the primary source of aromatic stabilization. CCs and CCSs however, are reliable aromaticity indices for monocyclic π -systems²⁹. In general, ring current maps are obtained by superposing all the CCs onto the molecule using Eq. 3. The magnitude and the direction of the current intensity induced in the mobile π -electrons by the magnetic field are presented in Figure 4, where the intensities of all π -electron currents are given in the units which are induced in the benzene ring. Here, diamagnetic circulation is shown as counterclockwise, paramagnetic as clockwise. As shown in figure 4, all the compounds sustain a diatropic current along the macrocycle and it is bifurcated whenever it passes through a five-membered ring. In general, paramagnetic and diamagnetic currents flow in opposite directions on the outer C-C bonds of the five-membered rings and thus they partially cancel each other out in those rings. For the A and B rings in compound **1**, it can be seen that the preferred path of the current is through those C-C bonds in the A ring and through those C-N bonds in the B ring. For example, for the A ring in **1**, the strength of the current passing through the C-C bond ($1.369I_0$) is stronger than that passing through the C-N bonds ($0.664I_0$), whereas in the B ring, the current passing through the C-C bond ($0.390I_0$) is weaker than that through C-N bonds ($1.643I_0$). Similar behavior is observed if the B, C, and D rings in **2a**, **2b**, and **2c** are analyzed. This observation gives support for the earlier surmise that in porphyrin, the main current selects the outer pathway in those five-membered rings which contain an –NH– group, and it selects the inner pathway in those five-membered rings which do not contain an –NH– group⁵¹.

For the A ring in **2a**, the presence of an -NH- group leads to a decrease in the current intensity while crossing the =N-NH- unit, and the current difference between the inner and outer sections becomes much smaller than in any other five-membered ring. This is attributable to the large paratropic contribution of circuit r_2 . For the A ring both in **2b** and **2c**, the strength of currents passing through the =N-N= unit is stronger than that passing through the -NH- group, whereas the current passing through the -N=N- unit is weaker than that through the -N= group. By comparing the CC values of A and C rings in **2a**, we found that the insertion of nitrogen atoms in ring A, which then becomes a triazole unit, decreases the diatropic ring current differential as it passes through both the =N-NH- unit and -N= group. However, by comparing the A rings of **2a** and **2b** we can see that the presence of =N-NH- and -N=N- units does not change the path-selecting nature of the current as it passes through the five-membered rings. That is to say, the path the main ring current selects does not contain an -NH- group. However, the insertion of nitrogen atoms in ring A, leads to a limited decrease in the macrocyclic ring current intensities of **2a**, **2b**, **2c**, and **3** when compared to **1**. In the case of **3** and **4**, the path of the main ring current runs along the macrocycle circuit located around the internal cross (r_7) and avoids the =N-N= unit and the C-C bonds. For all compounds shown in Fig. 4, the differential in the π -electron current through each individual ring is roughly proportional to the magnitude of the corresponding BRE values for those same rings, which are shown in Fig. 1. It can be seen above, that the graph-theoretical method of analysis is an important method in characterizing both the energetic and magnetic properties of polycyclic aromatic compounds.

4. Conclusion

The global aromaticity and the local aromaticity as well as the magnetic properties of triazolephorphyrazines were investigated using the graph-theoretical method. Important findings in this study are summarized as follows:

- 1) The global aromaticity of porphyrazine and of the triazolephorphyrazines is lower than that of porphyrin. This is due to these compounds not obeying the rule of topological charge stabilization. Macrocyclic conjugation never makes a major contribution to the global aromaticity of porphyrazine or to the triazolephorphyrazines. All these compounds are stabilized primarily by the local aromaticity of the smaller, five-membered circuits which contain an -NH- group. The local aromatic properties of five-membered circuits are related to the global properties of the compound. However, NICS(0) and HOMA values differ from the estimations of local aromaticity of our work.
- 2) For all molecules studied herein, as it passes through each five-membered ring, the larger diatropic π -electron current selects those C-C bond sections which contain an -NH- group, and those C-N bond sections which do not contain an -NH- group. The strength of the diatropic ring current when passing through the C-N bond sections which link two five-membered rings, exhibits relatively greater intensity than when passing through the five-membered ring sections.

ACKNOWLEDGMENTS

This work was financially supported by the Natural Science Foundation of China (No. 21262037), and by the Urumqi Science and Technology Project (No. H101133001) of the Xinjiang Uyghur Autonomous Region, China.

5. References

- 1 A. Jasat and D. Dolphin, *Chem. Rev.*, 1997, **97**, 2267.
- 2 T. D. Lash, *J. Porphyrins Phthalocyanines*, 2011, **15**, 1093.

- 3 M. Stepien, N. Sprutta and L. Latos-Grazyński, *Angew. Chem., Int. Ed.*, 2011, **50**, 4288.
- 4 M. K. Cyranski, T. M. Krygowski, M. Wiciorowski, N. J. R. v. E. Hommes and P. v. R. Schleyer, *Angew. Chem., Int. Ed.*, 1998, **37**, 177.
- 5 E. Steiner and P. W. Fowler, *ChemPhysChem*, 2002, **3**, 114.
- 6 J. Jusélius and D. Sundholm, *J. Org. Chem.* 2000, **65**, 5233.
- 7 H. Z. Hu and S. Y. Ma, *Int. J. Quantum. Chem.* 2010, 110, 1682.
- 8 E. A. Makarova and E. A. Lukyanets, *J. Porphyrins Phthalocyanines*, 2009, **13**, 188.
- 9 M. S. Rodríguez-Morgade and P. A. Stuzhin, *J. Porphyrins Phthalocyanines*, 2004, **8**, 1129.
- 10 H. Miwa, E. A. Makarova, K. Ishii, E. A. Luk'yanets and N. Kobayashi, *Chem. Eur. J.*, 2002, **8**, 1082.
- 11 V. I. Minkin, M. N. Glukhovtsev and B. Y. Simkin, *Aromaticity and Antiaromaticity: Electronic and Structural Aspects*, Wiley, New York, 1994.
- 12 J. Kruszewski and T. M. Krygowski, *Tetrahedron Lett.*, 1972, **13**, 3839.
- 13 T. M. Krygowski, *J. Chem. Inf. Comput. Sci.*, 1993, **33**, 70.
- 14 P. v. R. Schleyer, C. Maerker, A. Dransfeld, H. Jiao and N. J. R. V. E. Hommes, *J. Am. Chem. Soc.*, 1996, **118**, 6317.
- 15 G. Merino, A. Vela and T. Heine, *Chem. Rev.*, 2005, **105**, 3812.
- 16 R. Islas, T. Heine and G. Merino, *Acc. Chem. Res.* 2012, **45**, 215.
- 17 G. Merino, T. Heine and G. Seifert, *Chem. Eur. J.* 2004, **10**, 4367.
- 18 Z. F. Chen, C. S. Wannere, C. Corminboeuf, R. Puchta and P. v. R. Schleyer, *Chem. Rev.*, 2005, **105**, 3842.
- 19 J. Poater, X. Fradera, M. Duran and M. Solà, *Chem. Eur. J.*, 2003, **9**, 400.
- 20 J. Poater, M. Duran, M. Solà and B. Silvi, *Chem. Rev.*, 2005, **105**, 3911.
- 21 M. Mandado, N. Otero and R. A. Mosquera *Tetrahedron*, 2006, **62**, 12204.
- 22 J. Aihara, *J. Am. Chem. Soc.* 1976, **98**, 2750.
- 23 I. Gutman, M. Milun and N. Trinajstić, *J. Am. Chem. Soc.*, 1977, **99**, 1692.
- 24 B. Mohar and N. Trinajstić, *J. Comput. Chem.* 1982, **3**, 28.
- 25 R. Sekine, Y. Nakagami, and J. Aihara, *J. Phys. Chem. A* 2011, **115**, 6724.
- 26 P. Bultinck, S. Fias and R. Ponec, *Chem. Eur. J.* 2006, **12**, 8813.
- 27 S. Fias, S. V. Damme and P. Bultinck, *J. Comput. Chem.* 2008, **29**, 358.
- 28 S. Fias, S. V. Damme and P. Bultinck, *J. Comput. Chem.* 2010, **31**, 2286.
- 29 K. Najmidin, A. Kerim, P. Abdirishit, H. Kalam and T. Tawar, *J. Mol. Model.* 2013, **19**, 3529.
- 30 H. Fallah-Bagher-Shaidaei, C. S. Wannere, C. Corminboeuf, R. Puchta and P. v. R. Schleyer, *Org. Lett.*, 2006, **8**, 863.
- 31 A. C. Castro, E. Osorio, J. O. C. Jimenez-Halla, E. Matito, W. Tiznado and G. Merino (2010) *J. Chem. Theory. Comput.*, 2010, **6**, 2701.
- 32 C. Corminboeuf, T. Heine, G. Seifert, P. v. R. Schleyer and J. Weber, *Phys. Chem. Chem. Phys.*, 2004, **6**, 273.
- 33 M. K. Islyaikin, V. R. Ferro and J. M. García de la Vega, *J. Chem. Soc., Perkin Trans. 2*, 2002, 2104.
- 34 M. K. Islyaikin and E. A. Danilova, *Russ. Chem. Bull., Int. Ed.*, 2007, **56**, 689.
- 35 O. G. Khelevina, V. R. Ferro, M. K. Islyaikin, E. A. Veselkova, M. G. Stryapan and J. M. García de la Vega, *J. Phys. Org. Chem.* 2005, **18**, 329.
- 36 J. Aihara, *Bull. Chem. Soc. Jpn.*, 2004, **77**, 651.
- 37 J. Aihara and H. Kanno, *J. Phys. Chem. A*, 2007, **111**, 8873.

- 38 J. Aihara, *J. Am. Chem. Soc.*, 1995, **117**, 4130.
- 39 J. Aihara, T. Ishida and H. Kanno, *Bull. Chem. Soc. Jpn.*, 2007, **80**, 1518.
- 40 J. Aihara, *J. Chem. Soc. Perkin Trans. 2*, 1996, 2185.
- 41 J. Aihara, *J. Am. Chem. Soc.*, 2006, **128**, 2873.
- 42 M. Makino and J. Aihara, *Phys. Chem. Chem. Phys.*, 2008, **10**, 591.
- 43 J. Aihara, *J. Am. Chem. Soc.* 1979, **101**, 5913.
- 44 J. Aihara and T. Horikawa, *Bull. Chem. Soc. Jpn.* 1983, **56**, 1853.
- 45 J. Aihara, *Chem. Phys. Lett.* 1983, **95**, 561.
- 46 J. Aihara, E. Kimura and T. M. Krygowski, *Bull. Chem. Soc. Jpn.* 2008, **81**, 826.
- 47 F. A. Van-Catledge, *J. Org. Chem.*, 1980, **45**, 4801.
- 48 B. M. Gimarc, *J. Am. Chem. Soc.*, 1983, **105**, 1979.
- 49 R. Arkin and A. Kerim, *Chem. Phys. Lett.*, 2012, **546**, 144.
- 50 H. Furuta, H. Maeda and A. Osuka, *J. Org. Chem.*, 2001, **66**, 8563.
- 51 H. Fliegl and D. Sundholm, *J. Org. Chem.* 2012, **77**, 3408.

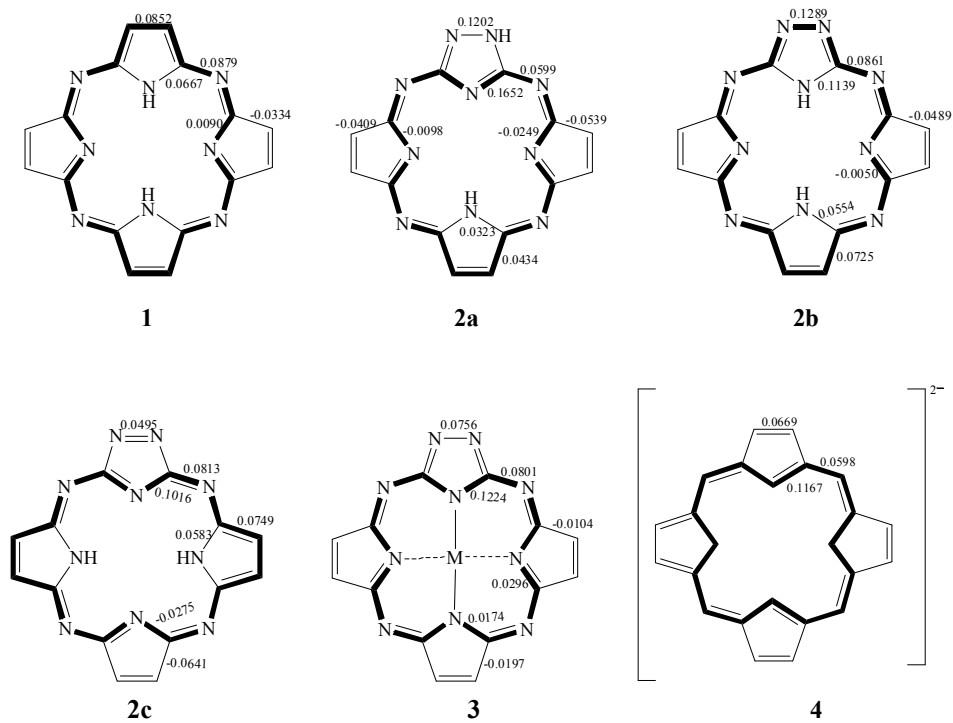


Figure 1. BRE values for PA (**1**), three tautomers of TAPs (**2a**, **2b**, **2c**), metalloTAP (**3**), and for the URF (**4**). The molecular fragments corresponding to the annulene-like substructure predicted by the CRE values are represented in bold.

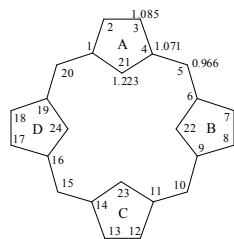
**5**

Figure 2. Labeling and π -electron density in the URFs for compounds 1-4.

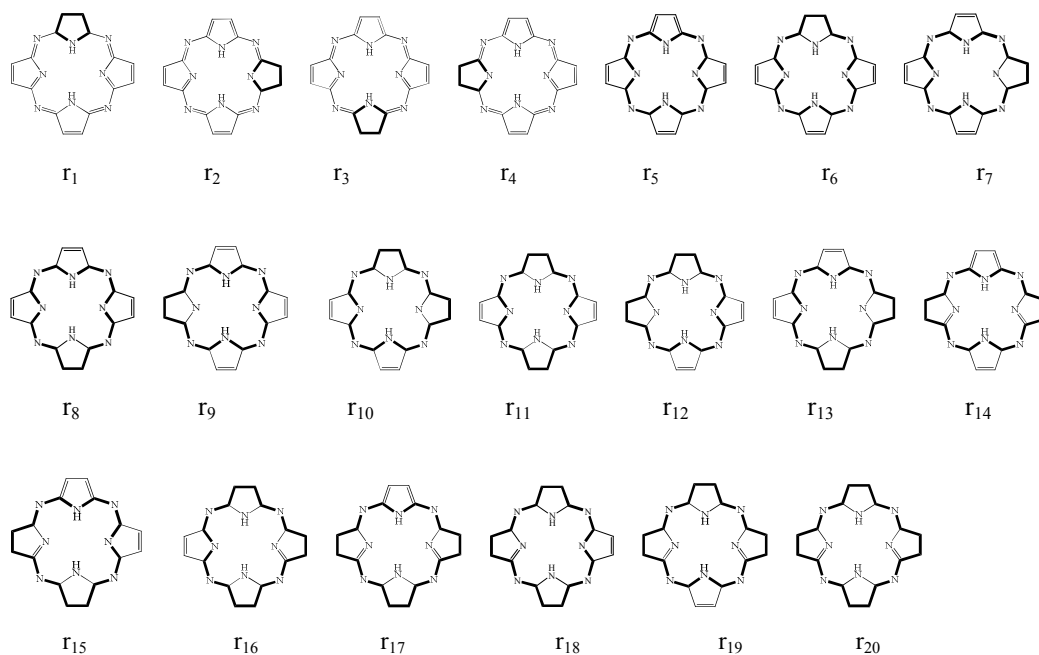


Figure 3. Non-Identical Circuits in PA

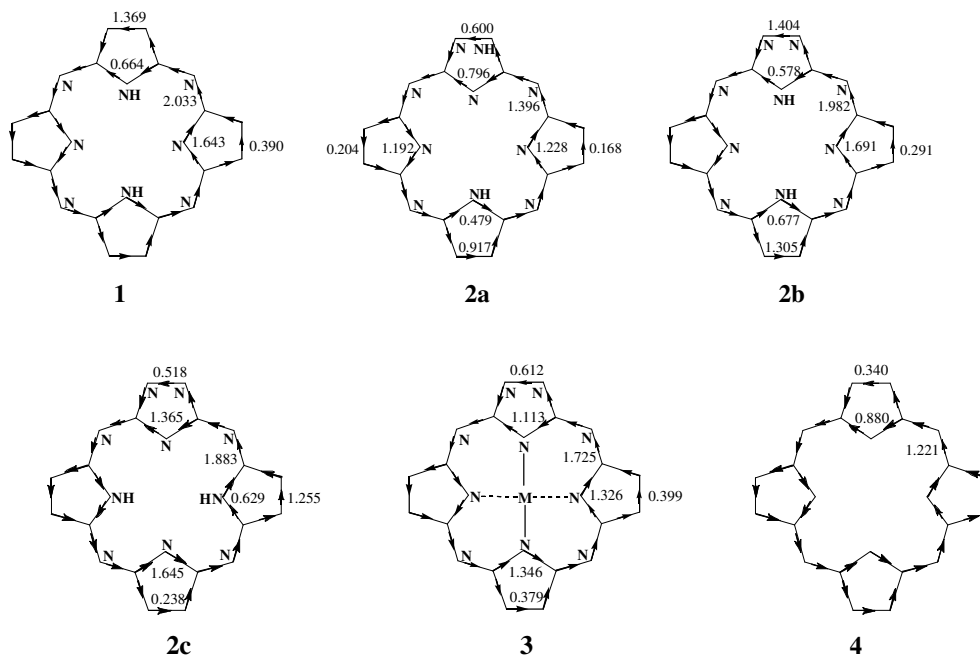


Fig. 4. π -Current density map for PA and related species.